Journal of the Serbian Chemical Society
JSCS@tmf.bg.ac.rs • www.shd.org.rs/JSCS
J. Serb. Chem. Soc. *89* (10) 1311–1321 (2024)
JSCS–5789
Original scientific paper
Published 2 November, 2024

Molecular dynamics modelling of the structural, dynamic and dielectric properties of the LiF–ethylene carbonate energy storage system at various temperatures

SANAA RABII, AYOUB LAHMIDI, SAMIR CHTITA, MHAMMED EL KOUALI, MOHAMMED TALBI and ABDELKBIR ERROUGUI*

Laboratory of Analytical and Molecular Chemistry, Faculty of Sciences Ben M'Sick, Hassan II University of Casablanca, Morocco

(Received 5 February, revised 21 March, accepted 16 June 2024)

Abstract: Lithium-ion batteries (LIBs) play a vital role in advancing the hybrid industry, especially in electric vehicles, as clean and sustainable electrochemical energy sources. However, the prevalent use of organic solvents in the liquid electrolytes of these energy storage systems raises environmental concerns. In this study, we investigated the impact of a polar aprotic solvent, ethylene carbonate (EC), on the structural, dynamic and dielectric properties of the LiF electrolyte using molecular dynamics simulations. By employing the CHARMM 36 force field, our goal was to comprehend the various physicochemical phenomena occurring in this electrolytic system across different temperatures within the saturation region. The structural properties were analyzed through the computation of the radial distribution function (*RDF*) for various pairs, while the dynamic and dielectric behaviors were elucidated by simulating the self-diffusion coefficient (D) and the dielectric constant (ε).

Keywords: molecular dynamics; energy storage; solvation phenomenon; lithium fluoride; ethylene carbonate; lithium-ion batteries.

INTRODUCTION

Energy storage is at the heart of today's challenges because it is an essential element for the evolution towards a more sustainable, reliable, and profitable energy future.[1] It modulates energy production and consumption by reducing waste and storing excess energy when available, releasing it during periods of higher demand.[2] This capability proves particularly useful in compensating for the intermittency or fluctuation of renewable energy production, thereby meeting a constant demand.[3] Various forms of energy, including thermal, chemical, mechanical and electrical energy.[4,5] Energy storage technologies are diverse and

* Corresponding author. E-mail: Abdelkbir.errougui@univh2c.ma
https://doi.org/10.2298/JSC240205061R

encompass batteries, systems such as flywheels, springs, gravity energy storage systems and pumped hydraulic storage.[6]

Rechargeable lithium-ion batteries (LIBs) stand out as one of the most versatile battery systems, exhibiting significant improvements in energy density and efficiency. They find wide applications in electronic devices, such as laptops and mobile phones, and are crucial for storing the energy required to power electric vehicles.[7–12] Furthermore, the performance of rechargeable lithium batteries is strongly influenced by the nature of the chosen electrolyte and the understanding of the different mechanisms at play within the electrolyte solution in the presence of an organic solvent. Presently, new materials utilized as cathodes or anodes necessitate solvate electrolytes to ensure the highest possible conductivity and ion mobility between electrodes.[13,14]

The objective of this study is to use the molecular dynamics approach to simulate the structural, dynamic and dielectric behavior of the LiF–ethylene carbonate (EC) system, and then understanding the effect of temperature on the solvation mechanism of Li^+ and F^- in the presence of an organic aprotic solvent namely EC widely used in lithium battery technology, it can also be used in other applications as plasticizer and precursor of vinylene carbonate, and it is present in fibers, plastics, surface coatings, and dyes.[15,16]

The present article is a continuation of our previous work focused on molecular simulations.[17–19] Literature analysis has shown that this LiF–EC energy storage system is very little studied, especially in the temperature range from 313.15 to 373.15 K, which is the subject of our simulations using the molecular dynamics approach.

COMPUTATIONAL DETAILS

The molecular dynamics (MD) simulations approach is one of the powerful and appropriate methods to study the properties of the LiF–EC energy storage system due to its precision, its ability to provide a detailed understanding of molecular interactions, its flexibility, its numerous applications, and its capacity for validation through experimentation. The GROMACS--2020-6 software package was employed to conduct radial distribution function (RDF), self-diffusion coefficient and dielectric constant calculations, allowing for the extraction of the structural, dynamic and dielectric properties of this system over a wide range of temperatures.[20,21] In this work, all simulations were performed using the CHARMM force field.[22,23]

The values of the charges and intermolecular interactions between the solvent molecules, Li^+ and F^- are described with the Lennard–Jones (LJ) parameters (Table I). The Ewald summation method was used to calculate electrostatic interactions.[24,25]

After the optimization process, the following dynamics simulation procedures are performed, NVT equilibration was executed to control the temperature for this system using Nose––Hoover thermostat.[26,27] After that, NPT equilibration was done using Parrinello–Rahman barostat[28] at 1 bar for 60 ns. All these simulations were conducted with a time-step of 1 fs.

The simulation was conducted with 803 EC solvent molecules, and the concentration of the system is 0.9 M LiF salt, corresponding to 68 Li^+ and 68 F^- in a simulation box of (5×5×5) nm^3, with temperatures ranging from 313.15 to 373.15 K.

In addition, our previous research[29,30] elaborates on the theoretical and mathematical approaches employed to analyze all properties calculated in this work.

TABLE I. Lennard–Jones and electrostatic parameters for the EC solvent[31]; O_1: oxygen of ethylene carbonate cycle, C_1: carbon of ethylene carbonate cycle, O_2: Oxygen of carbonyl group, C_2: carbone of carbonyl group

Element	q(e)	σ_{LJ} / nm	ε_{LJ} / kJ/mol
Li^+	+1.000	0.2311	0.0097
F^-	–1.000	0.2513	0.5648
O_1	–0.4684	0.3153	0.6363
C_1	0.0330	0.3875	0.2301
O_2	0.6452	0.3029	0.5021
C_2	1.0996	0.3563	0.4602
H	0.1041	0.2351	0.0920

RESULTS AND DISCUSSION

Thermodynamics and solvation properties

The structural properties of the electrolytic system involving lithium fluoride dissolved in the aprotic solvent ethylene carbonate (EC) were determined through molecular simulation. This was achieved by calculating the radial distribution function (*RDF*), which evaluates the structural behavior of various pairs: ion–ion, ion–solvent and solvent–solvent. The interatomic distance and the degree of coordination were also calculated. Table II presents the solvation's structural and thermodynamic properties for this electrolytic system at different temperatures ranging from 313.15 to 373.15 K.

TABLE II. Simulation values of thermodynamics and structural properties of LiF–EC energy storage system at various temperatures

LiF–EC system for 0.9 M	1	2	3	4	5	6	Reference
Temperature, K	313.15	323.15	333.15	343.15	353.15	373.15	–
Volume, nm^3	96.704	97.499	98.203	99.039	99.883	101.446	–
Density, 10^3 kg m^{-3}	1.244	1.234	1.225	1.215	1.204	1.186	1.320 for EC[32]
E_{kin} / 10^3 kJ mol^{-1}	27.705	28.591	29.476	30.363	31.247	33.015	–
$r_{max(Li-O2)}$ / nm	0.19	0.19	0.19	0.19	0.19	0.19	0.19[32]
Coordination number (CN_{Li-O2})	1.81	1.67	1.57	1.48	1.33	1.29	–
$r_{max(F-H)}$ / nm	0.25	0.25	0.25	0.25	0.25	0.25	–
Coordination number (CN_{F-H})	2.48	2.45	2.36	2.23	2.13	2.10	–
$r_{max(Li-F)}$ / nm	0.18	0.18	0.18	0.18	0.18	0.18	0.17[34]
Coordination number (CN_{LiF})	2.23	2.59	2.66	2.83	3.14	3.19	–
$r_{max(O2-H)}$ / nm	0.20	0.20	0.20	0.20	0.20	0.20	0.28[32]
$r_{max(O2-O2)}$ / nm	0.38	0.38	0.38	0.38	0.38	0.38	0.39[32]

Fig. 1 illustrates that the density of the LiF–EC electrolyte system decreases as the temperature increases, with values ranging between 1.244 and 1.186 g cm^{-3}. Additionally, our molecular simulation results follow the same trend observed by

Chang *et al.* for the pure aprotic solvent EC.[32] Indeed, the observed difference is mainly due to the effect of adding the LiF electrolyte, which generates mutual interactions between the aprotic polar solvent (EC) and the ions (Li^+ and F^-) present in the electrolyte solution, leading to a noticeable decrease in density. In Fig. 2, the microstructure formed by organic solvent molecules is analyzed. The *RDF*s variation as a function of the interatomic distance for O–O in ethylene carbonate exhibits multiple peaks. The first layer, situated at a distance of 0.38 nm, indicates a maximization of intramolecular dipole interactions. The intensity decreases with rising temperature due to thermal agitation.[32,35]

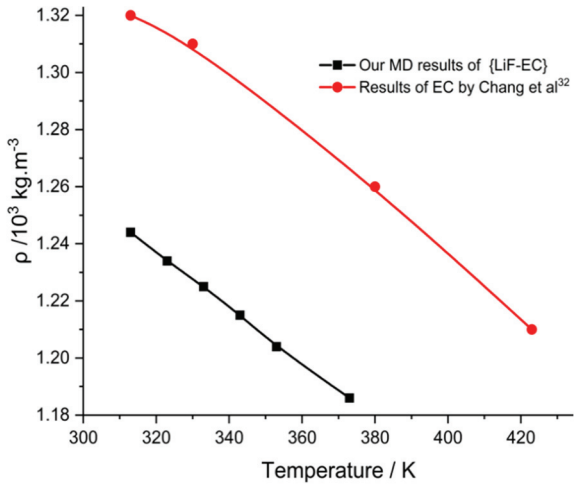

Fig. 1. Density simulations for the LiF–EC system at different temperatures.

Fig. 3 depicts the *RDF* for O_2–H. The temperature-disrupting effect is evident, showing a single peak at a distance of 0.20 nm. This interatomic distance is shorter compared to that found between O_2–O_2, suggesting that carbonyl oxygen has a preference for association with hydrogen atoms due to the attraction between O_2–H.[32,36]

Analysis of Fig. 4 reveals a prominent peak at a distance of 0.19 nm, suggesting a coordination number between 1.81 and 1.29 EC molecules around Li^+. This value is lower than those reported in classical simulations by Skarmoutsos *et al.*,[37] Smith and Borodin[38] and other theoretical studies.[39–41] Experimental studies generally indicate a coordination number of lithium between 4 and 5 in the presence of EC, with the highest value observed so far being $CN = 7$ in 1 M of $LiClO_4$ by Castriota *et al.*[42] Additionally, we found that lithium completes its coordination with F^- which compete with the oxygen of the carbonyl due to their high electronegativity. The absence of an acidic proton in the aprotic solvent, such as EC,

facilitates the penetration of fluoride. Consequently, lithium manages to complete its coordination with 5 species (2 EC molecules, and 3 F^-).

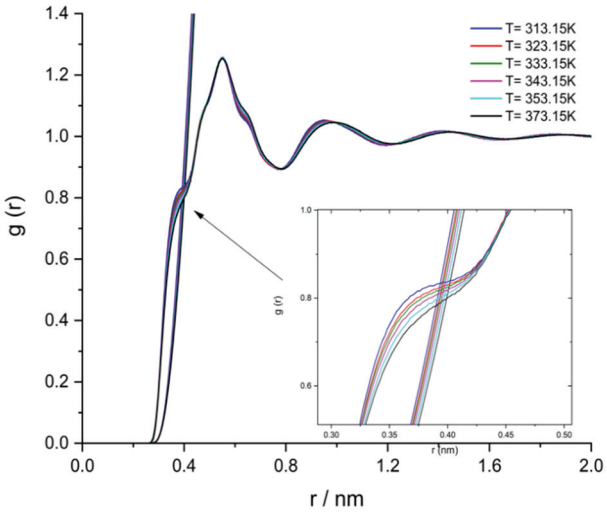

Fig. 2. Evolution of the $g_{O2\text{-}O2}(r)$ functions at different temperatures.

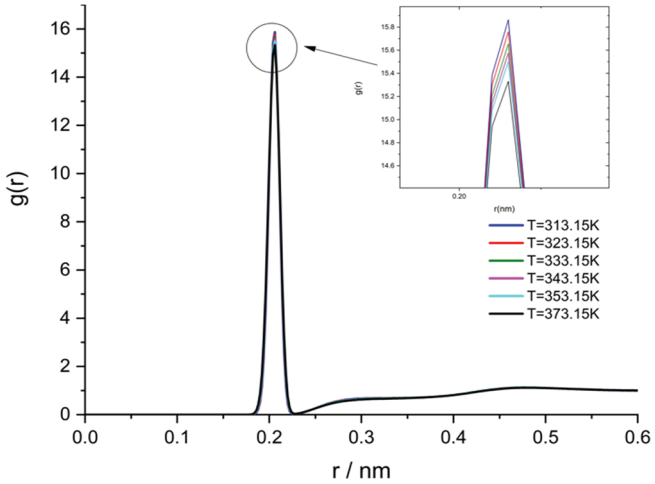

Fig. 3. Evolution of the $g_{O2\text{-}H}(r)$ functions at different temperatures.

Moreover, the distribution of F–H bonds is depicted in Fig. 5. This curve illustrates that F^- is predominantly surrounded by two hydrogen shells of EC molecules. The first shell, located at 0.25 nm, is broad and intense, resulting from the mutual polarizability of F^- and the solvent. Notably, there is no contribution to the solvation of the anions through hydrogen bonding, as the aprotic polar solvent's nature exclusively favors the solvation of Li^+. Consequently, F^- remains free and

unsolvated in the solution due to the absence of an acidic hydrogen atom. Additionally, the distribution of the F–H network undergoes significant degradation due to thermal agitation evolution, as observed by Castriota, Armand and Parker *et al.*[42–44]

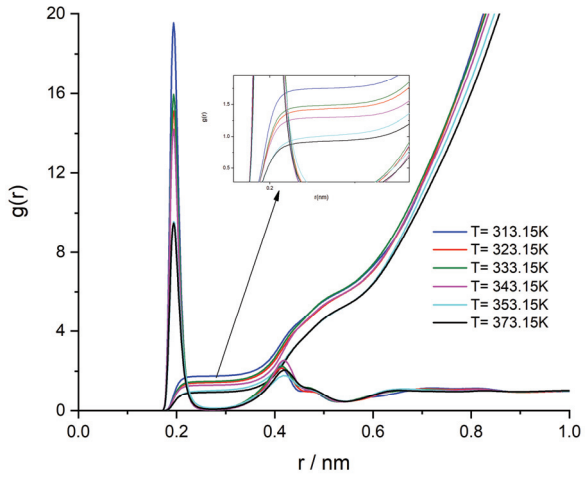

Fig. 4. Variation of the $g_{Li\text{-}O2}(r)$ functions at various temperatures.

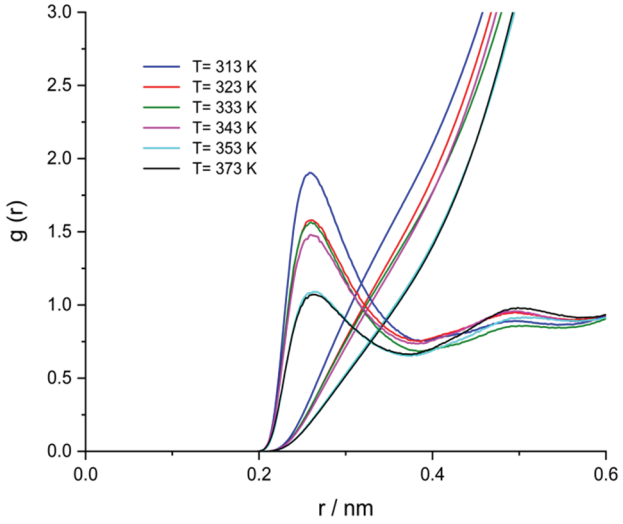

Fig. 5. Variation of the $g_{F\text{-}H}(r)$ functions at various temperatures.

The analysis of Fig. 6 reveals that the solvation process of the LiF electrolyte in the presence of an aprotic solvent primarily occurs in the form of pairs of contact ions. This process is evidently influenced by temperature evolution; specifically, an increase in temperature results in heightened intensity of *RDF* functions. This

is substantiated by the presence of a major and more intense peak at a distance of 0.18 nm, corresponding to the formation of a substantial number of contact ion pairs (CIP) in the electrolyte.[34] Consequently, this leads to the creation of successive shells formed by F^- around Li^+, attributed to the freedom of the anion and the aprotic polar behavior of the solvent, suggesting robust interactions between non-ionized ions, influenced by the solvent's polarity.

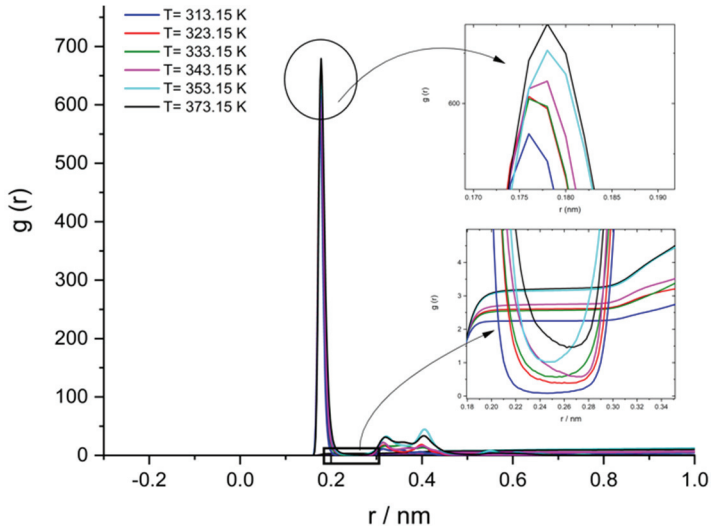

Fig. 6. Variation of the $g_{Li\text{-}F}(r)$ functions at various temperatures.

Moreover, our findings indicate that Li^+ is surrounded by 2.32 up to 3.19 F^-. This coordination variation is significantly impacted by thermal agitation, electronegativity difference in Li–F, as well as the size and charge, particularly of the fluorides.[45,46]

Dynamics and dielectric properties

In this study, we investigated the transport and dielectric properties of the electrolytic system LiF–EC at various temperatures for a concentration of 0.9 M using molecular dynamics simulations, as summarized in Table III.

TABLE III. Simulation results for the dynamical and dielectric properties of EC, Li^+ and F^- at various temperatures – the self-diffusion coefficient (10^{-9} m^2/s)

Temperature, K	DEC–LiF	DEC	DLi+	DF−	ε
313.15	0.202±0.002	0.206±0.002	0.046±0.004	0.050±0.003	59.67±0.34
323.15	0.287±0.003	0.293±0.003	0.057±0.017	0.071±0.022	54.88±0.43
333.15	0.364±0.003	0.372±0.003	0.055±0.003	0.069±0.005	56.03±0.59
343.15	0.451±0.006	0.459±0.007	0.092±0.004	0.126±0.005	58.52±0.24
353.15	0.628±0.009	0.641±0.007	0.113±0.075	0.116±0.074	61.82±0.48
373.15	0.812±0.005	0.829±0.007	0.139±0.071	0.145±0.067	57.20±0.07

The analysis of Fig. 7 illustrates that the self-diffusion coefficient increases with the evolution of the temperature. In addition, Li^+ and F^- move with almost the same speed during the simulation time, suggesting that this relative mobility is mainly due to the strong electrostatic interactions, the difference in electronegativity between the two ions ($\eta_{Li-F} = 3$), the size of the ions, and also the polar and aprotic nature of the solvent. These factors favor the formation of contact ion pairs and the reduction of ion–solvent interactions.[32,47,48]

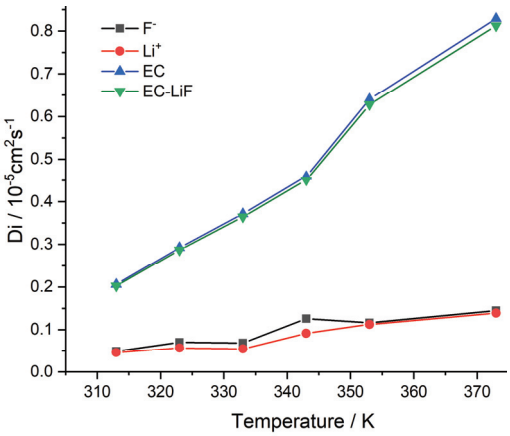

Fig. 7. Self-diffusion coefficients variation of the EC solvent, lithium and fluoride ions in the LiF–EC storage energetic system as a function of temperature.

Fig. 8 reveals that the temperature evolution influences the dielectric behavior of the electrolytic system; indeed, the dielectric constant decreases with an increase in temperature. Additionally, we observed a significant decrease in the dielectric constant of the pure solvent, dropping from 89.78 to 59.67 at $T = 313$ K.[49] This phenomenon can be explained by the disruptive effect of the LiF on the pure EC solvent. Furthermore, Parida *et al.* reported a similar behavior during the study of the energy system $LiPF_6$–EC.[33]

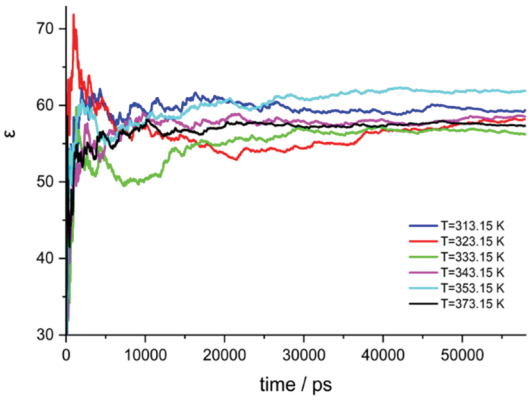

Fig. 8. Dielectric constant of the LiF–EC system at various temperatures.

CONCLUSION

In this study, we employed the molecular dynamics approach to simulate new structural, dynamic and dielectric properties of the innovative energy storage system LiF–ethylene carbonate, an electrolyte system with an ionic composition widely employed in lithium-ion battery technology. Specific algorithms were implemented based on the choice of a CHARMM force field, enabling the description of various ion–ion, ion–solvent and solvent–solvent interactions. The influence of temperature on structural behavior was assessed using the radial distribution function (*RDF*), which involved calculating the interatomic distance and coordination of various pairs within the solvation shells.

Furthermore, this scientific approach allowed us to enhance our understanding of different interactions and molecular mechanisms inherent in such an innovative energy storage system extensively used in rechargeable lithium battery technology. Temperature also plays a significant role in influencing the mobility and dielectric behavior of the current system, with its self-diffusion coefficient increasing as the temperature rises. Notably, the solvent was found to have a minimal impact on ion diffusion. The molecular simulation results obtained will offer valuable information for designing new materials and improving our comprehension of the processes governing this type of electrolytic energy storage systems.

ИЗВОД

МОДЕЛОВАЊЕ СТРУКТУРНИХ, ДИНАМИЧКИХ И ДИЕЛЕКТРИЧНИХ СВОЈСТАВА СИСТЕМА LiF–ЕТИЛЕН-КАРБОНАТ ЗА СКЛАДИШТЕЊЕ ЕНЕРГИЈЕ МОЛЕКУЛСКОМ ДИНАМИКОМ НА РАЗЛИЧИТИМ ТЕМПЕРАТУРАМА

SANAA RABII, AYOUB LAHMIDI, SAMIR CHTITA, MHAMMED EL KOUALI, MOHAMMED TALBI и ABDELKBIR ERROUGUI

Laboratory of Analytical and Molecular Chemistry, Faculty of Sciences Ben M'Sick, Hassan II University of Casablanca, Morocco

Литијум-јонске батерије играју важну улогу у развоју индустрије хибрида, посебно у случају електричних возила, као чисти и одрживи електрохемијски извори енергије. Међутим, преовлађујућа употреба органских растварача у течним електролитима ових система за складиштење енергије изазива забринутост за животну средину. У овом раду, испитиван је утицај поларног апротичног растварача, етилен-карбоната, на структурна, динамичка и диелектрична својства LiF електролита применом симулација молекулске динамике. Применом CHARMM 36 поља сила, циљ је био да се објасне различити физичкохемијски феномени који се јављају у овом електролитичком систему на различитим температурама у области засићења. Структурне особине су анализиране кроз прорачуне радијалне дистрибуционе функције за различите парове, док су динамичко и дилектрично понашање разјашњени симулацијама коефицијента самодифузије и диелектричне константе.

(Примљено 5. Фебруара, ревидирано 21. марта, прихваћено 16. јуна 2024)

REFERENCES

1. I. Hadjipaschalis, A. Poullikkas, V. Efthimiou, *Renew. Sust. Energy Rev.* **13** (2009) 1513 (https://doi.org/10.1016/j.rser.2008.09.028)

2. A. Kusko, J. Dedad, *IEEE Ind. Appl. Mag.* **13** (2007) 66 (https://doi.org/10.1109/MIA.2007.4283511)
3. T. M. I. Mahlia, T. J. Saktisahdan, A. Jannifar, M. H. Hasan, H. S. C. Matseelar, *Renew. Sust. Energy Rev.* **33** (2014) 532 (https://doi.org/10.1016/j.rser.2014.01.068)
4. H. Ibrahim, A. Ilinc, in *Energy Storage – Technologies and Applications*, A. Zobaa, Ed., InTech, Rijeka, 2013 (https://doi.org/10.5772/52220)
5. D. Lefebvre, F. H. Tezel, *Renew. Sust. Energy Rev.* **67** (2017) 116 (https://doi.org/10.1016/j.rser.2016.08.019)
6. S. Hameer, J. L. Van Niekerk, *Int. J. Energy Res.* **39** (2015) 1179 (https://doi.org/10.1002/er.3294)
7. S. Chen, C. Niu, H. Lee, Q. Li, L. Yu, W. Xu, J.-G. Zhang, E. J. Dufek, M. S. Whittingham, S. Meng, J. Xiao, J. Liu, *Joule* **3** (2019) 1094 (https://doi.org/10.1016/j.joule.2019.02.004)
8. O. Salihoglu, R. Demir-Cakan, *J. Electrochem. Soc.* **164** (2017) A2948 (https://doi.org/10.1149/2.0271713jes)
9. X.-B. Cheng, C. Yan, J.-Q. Huang, P. Li, L. Zhu, L. Zhao, Y. Zhang, W. Zhu, S.-T. Yang, Q. Zhang, *Energy Storage Mater.* **6** (2017) 18 (https://doi.org/10.1016/j.ensm.2016.09.003)
10. H. Li, *Joule* **3** (2019) 911 (https://doi.org/10.1016/j.joule.2019.03.028)
11. C. Niu, H. Lee, S. Chen, Q. Li, J. Du, W. Xu, J.-G. Zhang, M. S. Whittingham, J. Xiao, J. Liu, *Nat. Energy* **4** (2019) 551 (https://doi.org/10.1038/s41560-019-0390-6)
12. J. Y. Hwang, S. J. Park, C. S. Yoon, Y. K. Sun, *Energy Environ. Sci.* **12** (2019) 2174 (https://doi.org/10.1039/C9EE00716D)
13. A. Arslanargin, A. Powers, T. L. Beck, S. W. Rick, *J. Phys. Chem. B* **120** (2016) 1497 (https://doi.org/10.1021/acs.jpcb.5b06891)
14. X. You, M. I. Chaudhari, S. B. Rempe, L. R. Pratt, *J. Phys. Chem., B* **120** (2016) 1849 (https://doi.org/10.1021/acs.jpcb.5b09561)
15. X. Li, G. Cheruvally, J. K. Kim, J. W. Choi, J.-H. Ahn, K. W. Kim, H. J. Ahn, *J. Power Sources* **167** (2007) 491 (https://doi.org/10.1016/j.jpowsour.2007.02.032)
16. L. Long, S. Wang, M. Xiao, Y. Meng, *J. Mater. Chem., A* **4** (2016) 10038 (https://doi.org/10.1039/C6TA02621D)
17. A. Errougui, M. Talbi, M. Kouali, *J. E3S Web Conf.* **297** (2021) 01009 (https://doi.org/10.1051/e3sconf/202129701009)
18. A. Errougui, A. Lahmidi, S. Chtita, M. El Kouali, M. Talbi, *J. Solution Chem.* **52** (2023) 176 (https://doi.org/10.1007/s10953-022-01222-7)
19. A. Lahmidi, S. Rabii, S. Chtita, M. E. Kouali, M. Talbi, A. Errougui, *Chem. Phys. Impact* **8** (2024) 100400 (https://doi.org/10.1016/j.chphi.2023.100400)
20. B. Hess, C. Kutzner, D. Van Der Spoel, E. Lindahl, *J. Chem. Theory Comput.* **4** (2008) 435 (https://doi.org/10.1021/ct700301q)
21. M. J. Abraham, T. Murtola, R. Schulz, S. Páll, J. C. Smith, B. Hess, E. Lindahl, *SoftwareX* **1**–**2** (2015) 19 (https://doi.org/10.1016/j.softx.2015.06.001)
22. B. R. Brooks, C. L. Brooks, A. D. Mackerell, L. Nilsson, R. J. Petrella, B. Roux, Y. Won, G. Archontis, C. Bartels, S. Boresch, A. Caflisch, L. Caves, Q. Cui, A. R. Dinner, M. Feig, S. Fischer, J. Gao, M. Hodoscek, W. Im, K. Kuczera, T. Lazaridis, J. Ma, V. Ovchinnikov, E. Paci, R. W. Pastor, C. B. Post, J. Z. Pu, M. Schaefer, B. Tidor, R. M. Venable, H. L. Woodcock, X. Wu, W. Yang, D. M. York, M. Karplus, *J. Comput. Chem*. **30** (2009) 1545 (https://doi.org/10.1002/jcc.21287)
23. P. Bjelkmar, P. Larsson, M. A. Cuendet, B. Hess, E. Lindahl, *J. Chem. Theory Comput.* **6** (2010) 459 (https://doi.org/10.1021/ct900549r)

24. T. Darden, D. York, L. Pedersen, *J. Phys. Chem.* **98** (1993) 10089 (https://doi.org/10.1063/1.464397)
25. U. Essmann, L. Perera, M. L. Berkowitz, T. Darden, H. Lee, L. G. Pedersen, *J. Phys. Chem.* **103** (1995) 8577 (https://doi.org/10.1063/1.470117)
26. M. Parrinello, A. Rahman, *J. Appl. Phys.* **52** (1981) 7182 (https://doi.org/10.1063/1.328693)
27. S. Nosé, *Mol. Phys.* **52** (1984) 255 (https://doi.org/10.1080/00268978400101201)
28. W. G. Hoover, *Phys. Rev., A* **31** (1985) 1695 (https://doi.org/10.1103/PhysRevA.31.1695)
29. A. Errougui, M. Talbi, M. El Kouali, *Egypt. J. Chem.* **65** (2022) 1 (https://doi.org/10.21608/ejchem.2021.67302.3453)
30. A. Lahmidi, S. Rabii, A. Errougui, S. Chtita, M. E. Kouali, M. Talbi, *J. Serb. Chem. Soc.* **89** (2024) 877 (https://doi.org/10.2298/JSC231106003L)
31. D. Ward, R. Jones, J. Templeton, K. Reyes, M. Kane, *ECS Trans.* **61** (2014) 181 (https://doi.org/10.1149/06127.0181ecst)
32. T.-M. Chang, L. X. Dang, *J. Phys. Chem.* **147** (2017) 161709 (https://doi.org/10.1063/1.4991565)
33. R. Parida, S. Pahari, M. Jana, *J. Power Sources* **521** (2022) 230962 (https://doi.org/10.1016/j.jpowsour.2021.230962)
34. B. Ravikumar, M. Mynam, S. Repaka, B. Rai, *J. Mol. Liq.* **338** (2021) 116613 (https://doi.org/10.1016/j.molliq.2021.116613)
35. J.-C. Soetens, C. Millot, B. Maigret, I. Bakó, *J. Mol. Liq.* **92** (2001) 201 (https://doi.org/10.1016/S0167-7322(01)00192-1)
36. L. B. Silva, & L. C. G. Freitas, *J. Mol. Struct: Theochem* **806** (2007) 23 (https://doi.org/10.1016/j.theochem.2006.10.014)
37. I. Skarmoutsos, V. Ponnuchamy, V. Vetere, S. Mossa, *J. Phys. Chem., C* **119** (2015) 4502–4515 (https://doi.org/10.1021/jp511132c)
38. O. Borodin, G. D. Smith, *J. Phys. Chem., B* **110** (2006) 4971 (https://doi.org/10.1021/jp056249q)
39. O. Borodin, G. D. Smith, *J. Phys. Chem., B* **113** (2009) 1763 (https://doi.org/10.1021/jp809614h)
40. P. Ganesh, D. Jiang, P. R. C. Kent, *J. Phys. Chem., B* **115** (2011) 3085 (https://doi.org/10.1021/jp2003529)
41. K. Leung, C. M. Tenney, *J. Phys. Chem., C* **117** (2013) 24224 (https://doi.org/10.1021/jp408974k)
42. M. Castriota, E. Cazzanelli, I. Nicotera, L. Coppola, C. Oliviero, G. A. Ranieri, *J. Phys. Chem.* **118** (2003) 5537 (https://doi.org/10.1063/1.1528190)
43. M. Armand, P. Touzain, *Mater. Sci. Eng.* **31** (1977) 319 (https://doi.org/10.1016/0025-5416(77)90052-0)
44. A. J. Parker, *Q. Rev. Chem. Soc.* **16** (1962) 163 (https://doi.org/10.1039/QR9621600163)
45. J. Jones, M. Anouti, M. Caillon-Caravanier, P. Willmann, D. Lemordant, *Fluid Phase Equilib.* **285** (2009) 62 (https://doi.org/10.1016/j.fluid.2009.07.020)
46. S. Wang, Z. Tan, L. Sun, S. Xiao, W.Hu, H. Deng, *J. Mol. Liq.* **369** (2023) 120833 (https://doi.org/10.1016/j.molliq.2022.120833)
47. X. You, M. I. Chaudhari, S. B. Rempe, L. R. Pratt, *J. Phys. Chem., B* **120** (2016) 1849 (https://doi.org/10.1021/acs.jpcb.5b09561)
48. A. Rodriguez, S. T. Lam, M. Hu, *ACS Appl. Mater. Interfaces* **13** (2021) 55367 (https://doi.org/10.1021/acsami.1c17942)
49. R. Payne, I. E. Theodorou, *J. Phys. Chem.* **76** (1927) 2892 (https://doi.org/10.1021/j100664a019).